Environmental Pollution 363 (2024) 125212

Contents lists available at ScienceDirect

Environmental Pollution

journal homepage: www.elsevier.com/locate/envpol

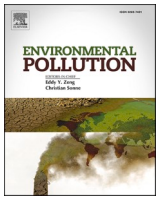

Identification and seasonal variation of $PM_{2.5}$-bound organophosphate flame retardants from industrial parks and the associated human health risk☆

Helong Ren [a,b], Qiang Chen [c], Zhaofa Huang [a,b], Yuhuan Zhu [c], Jing She [c], Yingxin Yu [a,b,*]

[a] Guangdong-Hong Kong-Macao Joint Laboratory for Contaminants Exposure and Health, Guangdong Key Laboratory of Environmental Catalysis and Health Risk Control, Institute of Environmental Health and Pollution Control, Guangdong University of Technology, Guangzhou, 510006, PR China
[b] Guangzhou Key Laboratory of Environmental Catalysis and Pollution Control, Key Laboratory of City Cluster Environmental Safety and Green Development, School of Environmental Science and Engineering, Guangdong University of Technology, Guangzhou, 510006, PR China
[c] College of Atmospheric Sciences, Lanzhou University, Lanzhou, 730000, PR China

ARTICLE INFO

Keywords:
Fine particles
Flame retardant
Composition profile
Source identification
Health risk assessment

ABSTRACT

Organophosphate flame retardants (OPFRs) have become pervasive environmental pollutants. However, there is a lack of information available regarding $PM_{2.5}$-bound OPFRs emitted from industrial parks dedicated to the manufacturing and processing of metal-related products. In this study, 15 OPFRs in $PM_{2.5}$ were identified from two industrial parks specializing in aluminum products and the deep processing of metals, respectively. The seasonal variations and health risks of OPFRs were investigated. The $PM_{2.5}$ and OPFR concentrations were 26.0–203 μg/m^3 and 12.4–6.38 × 10^4 pg/m^3, respectively. The OPFRs concentrations in the aluminum-processing industrial park exceeded those found in the metal-fabrication industrial park. Among the chloro-, aryl-, and alkyl-substituted OPFRs (i.e., Cl-OPFRs, aryl-OPFRs, and alkyl-OPFRs), Cl-OPFRs were the predominant homologues in the two parks (69.3% and 51.4%) and the control site. Tetraethyl diphosphate and tris(2-chloroethyl) phosphate were the most commonly occurring homologues in the aluminum and metal-fabrication industrial parks, respectively. Seasonal variations of the target OPFRs were observed, although there were slightly different concentrations between the sites. The correlation and principal component analyses with multiple linear regression identified metal waste disposal as the leading source of OPFRs in metal parks (68.0%), followed by traffic emissions (25.3%), adhesives and flame retardants in construction-related substances (3.82%), and mechanical emissions (2.85%). The health risk assessment showed that the hazard quotients for non-carcinogenic risk were <1, and the carcinogenic risks were <10^{-6}, which indicated that $PM_{2.5}$-bound OPFRs presented no obvious non-carcinogenic or carcinogenic risks. Comparatively, the notably elevated noncarcinogenic and carcinogenic risks associated with Cl-OPFRs highlighted the importance of enforcing strict emission regulations during the disposal of metal waste.

1. Introduction

Organophosphate flame retardants (OPFRs) are the successors to polybrominated diphenyl ethers and have been widely used in various electronics, plastics, and daily necessities (Van den Eede et al., 2011). It has been reported that the consumption of OPFRs in 2013 totaled approximately 620 kt, constituting approximately 30% of the overall global market share for flame retardants (Research In China, 2014). Organophosphate flame retardants are additives that do not form chemical bonds with the host material, enabling their constant release into the environment via processes such as evaporation, wear and tear, and seepage. They have received widespread attention due to their pervasive occurrence across a range of environmental matrices, including water, sediment, air, dust, and soil (Bekele et al., 2019; Ren et al., 2023; Zhong et al., 2021). These chemicals have even been detected within living organisms (Li et al., 2023; Yang et al., 2024).

☆ This paper has been recommended for acceptance by Admir Créso Targino.

* Corresponding author. Guangdong-Hong Kong-Macao Joint Laboratory for Contaminants Exposure and Health, Guangdong Key Laboratory of Environmental Catalysis and Health Risk Control, Institute of Environmental Health and Pollution Control, Guangdong University of Technology, Guangzhou, 510006, PR China.
E-mail address: yuyingxin@gdut.edu.cn (Y. Yu).

https://doi.org/10.1016/j.envpol.2024.125212
Received 9 August 2024; Received in revised form 7 October 2024; Accepted 26 October 2024
Available online 28 October 2024

Numerous toxicological studies conducted on various organisms have revealed a multitude of concerning effects associated with Tris (1, 3-dichloro-2-propyl) phosphate (TDCPP), Tris (2-chloroisopropyl) phosphate (TCIPP) (Li et al., 2023). These deleterious effects include hormonal interruption, neurological harm, liver toxicity, developmental toxicity, and interference with embryonic growth (Kim et al., 2019; Lu et al., 2023; Zeng et al., 2021).

Inhalation is one of the primary routes of human exposure to OPFRs. Fine particles ($PM_{2.5}$), with an aerodynamic diameter of less than or equal to 2.5 μm, is a major environmental concern (Montone et al., 2023; Thangavel et al., 2022). As semi-volatile compounds, OPFRs are prone to binding to $PM_{2.5}$ in the atmosphere, and have the propensity to penetrate deep into the lungs where they can trigger a cascade of adverse effects, including lung cancer and cardiovascular diseases (Lu et al., 2018). Several studies have demonstrated the widespread presence of OPFRs in $PM_{2.5}$, for example, in Pakistani e-waste recycling regions (Faiz et al., 2018) and large Chinese cities (Tansel, 2017; Zhao et al., 2021). A recent study has shown that $PM_{2.5}$-bound OPFRs are more persistent and can be transported for medium or long-distances (Sühring et al., 2016). Furthermore, Chen et al. (2020) found that $PM_{2.5}$-bound OPFRs could lead to the death of healthy lung epithelial cells and demonstrated significant redox activity in generating reactive oxygen species according to *in vitro* assays. Characterizing the potential health hazards of OPFRs in $PM_{2.5}$ is essential from both environmental and public health perspectives.

The release of OPFRs from industrial operations results in significant environmental contamination. For example, with the restriction and subsequent phasing out of polybrominated diphenyl ethers, OPFRs emerged as viable alternatives for use in electronic equipment. Industrial parks dedicated to the manufacturing, along with pyrometallurgical methods widely used to extract precious metals following board baking of metal-related products, are considered to be the primary or potential sources of OPFRs (Ma et al., 2021). However, there is little research available regarding $PM_{2.5}$-bound OPFRs emissions from these industrial sites. Several investigations have attempted to examine the origins of OPFRs through correlation and principal component analyses of specific OPFRs (Ge et al., 2020; Sanchez-Pinero et al., 2022). However, little quantitative data regarding source apportionment is available, especially for industrial sites where metal processing is conducted. It is important to determine the pollution concentrations, compositional characteristics, source apportionment, and potential health risks of OPFRs related to metal processing activities.

This study primarily investigated the temporal trends of $PM_{2.5}$-bound OPFRs and source apportionments, as well as the associated potential human health risks from metal processing activities in industrial parks dedicated to the manufacturing and processing of metal-related products. Atmospheric $PM_{2.5}$ samples were collected in both parks throughout four consecutive seasons, and 15 individual OPFRs were targeted as the primary compounds of interest. Therein, the first park mainly focuses on in-depth development and processing of the aluminum industry. It emphatically develops the comprehensive utilization industry of renewable resources, including high-value utilization of recycled steel and recycled aluminum. The second park mostly consists of the deep processing steel and rare earth new material sectors. It creates deep processing projects for seamless pipes, bars, wire rods, plates etc. The present study identified the sources of OPFRs in metal processing activities and assessed the health risks to exposed workers.

2. Materials and methods

2.1. Reagents and materials

The target 15 OPFR congeners, including 2-ethylhexyl diphenyl phosphate (EHDPP), tris(2-chloropropyl) phosphate (T (2-C)PP), tris(2-butoxyethyl) phosphate (TBOEP), tris(chloropropyl) phosphate (TCPP), tri-*o*-cresyl phosphate (*o*-TCP), tri-*p*-cresyl phosphate (*p*-TCP), TDCPP, tris(2-chloroethyl) phosphate (TCEP), tris(2-ethylhexyl) phosphate (TEHP), tetraethyl diphosphate (TEP), tributyl phosphate (TBP), triphenyl phosphate (TPhP), tripropyl phosphate (TPrP), TCIPP, and tri-*m*-cresyl phosphate (*m*-TCP) were sourced from AccuStandard (New Haven, CT, USA). Three deuterium-labeled OPFRs (TCEP-d_{12}, TPhP-d_{15}, and TBP-d_{27}) were also supplied by AccuStandard. High-performance liquid chromatography grade solvents, including ethyl acetate, dichloromethane, *n*-hexane, and *iso*-octane, were acquired from CNW (Duessedorf, Germany). Solid phase extraction cartridges were obtained from ANPEL Laboratory Technologies (Shanghai, China). Additionally, quartz fiber filter membranes (Whatman, Maidstone, UK) were used to sample $PM_{2.5}$, with each filter baked for 6 h at 450 °C prior to the sampling process.

2.2. Sample collection

The current study involved gathering $PM_{2.5}$ sample from an aluminum-processing industrial park (AP) (40.56° N, 110.12° E), a metal-fabrication industrial park (MP) (40.68° N, 109.74° E), and a control site (BH) (40.56° N, 109.92° E) in Baotou, Inner Mongolia Autonomous Region, China, in 2021. Sampling was conducted continuously over four seasons. In the AP, the capacity for recycling and processing scrap aluminum, steel, and rubber (plastic) was 225,000, 2000,000, and 100,000 t/a, respectively. One hundred different aluminum alloy deep-processed products were manufactured in the AP, including chemosynthesis aluminum-foil, aluminum wheels, architectural aluminum profiles, and aluminum alloy automobile parts. In the MP, steel smelting and smelting waste recycling were the main activities, and various rare earth metals, such as lanthanum, cerium, and neodymium, were formed by rare earth oxides after lava electrolysis. The BH is located nearby the studying area with similar climate and meteorological conditions, and the control site is generally less affected by industrial activities. Thus, we can better assess the impact of industrial activities on OPFRs in AP and MP by comparing them with the levels found in BH. The $PM_{2.5}$ samples were collected using quartz fiber filter membranes (90 mm, Whatman) via model 2034 medium-volume air samplers (Laoying, China) at 100 L/min for approximately 8 h (from 9:00 a.m. to 17:00 p.m.) at a height of approximately 1.5–2 m above the ground. A total of 77 p.m.$_{2.5}$ samples were collected. Table S1 presents the details of the sample data. The $PM_{2.5}$ samples were coated with aluminum foil and then sealed inside a bag. Finally, they were refrigerated at −20 °C until use.

2.3. Sample treatment and instrumental analysis

Following the addition of TCEP-d_{12}, TPhP-d_{15}, and TBP-d_{27} internal standards, each membrane was individually inserted into a Teflon centrifuge tube that held a 10 mL mixed solution of acetone, dichloromethane, and n-hexane (1:2:2, v/v). The mixture was then vortexed for 1 min. After 10 min of ultrasonic extraction, the sample was centrifuged at 2000 rpm. Chemicals were obtained following three extraction cycles. A copper sheet was added and the mixture was allowed to stand overnight. Afterward, the mixture of extracts was reduced to about 1 mL. The extract was then refined by passing it through a solid phase extraction cartridge that contained 1 g of Florisil, and OPFRs were eluted by 10 mL of ethyl acetate and dichloromethane (1:1, v/v). The eluents were blown to near dryness by a mild nitrogen stream, and the sample was rebuilt in 50 μL iso-octane and kept at −20 °C until further analysis.

The target OPFRs were measured using a gas chromatograph in conjunction with a triple quadrupole mass spectrometer (7890B-7000C, Agilent, Santa Clara, CA, USA). A DB-5MS capillary column (30 m × 0.25 mm × 0.25 μm) was used to separate OPFRs. The oven's programmed settings were as follows: after being held at 80 °C for 1 min, the temperature was increased to 300 °C at 10 °C/min (held for 5 min), then increased to 315 °C at 20 °C/min. Finally, the column temperature was maintained at 315 °C for 1 min. After adjusting the inlet

temperature to 280 °C, each injection of 1 μL of extract was analyzed. The carrier gas was high purity helium, which flowed continuously with an average velocity of 1 mL/min. The multiple reaction monitoring setting served as the MS acquisition mode. Table S2 provides a list of the monitored ions.

2.4. Quality assurance and quality control

A procedural blank was included in the analysis once every ten samples. For target analytes, the mean blank levels were less than 5% of the actual sample values. To confirm the detection accuracy, matrix-labeled samples combined with established concentrations of OPFRs were analyzed for each sample batch to determine the recovery efficiency (Zhang et al., 2023). All of the coefficient of determination (R^2) > 0.99 for the calibration curves indicated good linearity, and the target chemical concentrations were recovery- and blank-corrected. The three- and ten-fold signal to noise ratios were used to determine the limit of detection (LOD) and limit of quantification (LOQ) of each OPFR, respectively, because the procedure blanks contained almost no analytes (Ge et al., 2022). The LOD and LOQ ranged from 0.06 to 12.7 and 0.20–42.3 pg/m^3, respectively, as shown in Table S2.

2.5. Health risk assessment

In the present study, two toxic endpoints, i.e., noncarcinogenic risk (expressed as the hazard quotient (HQ)) and carcinogenic risk (CR), were used to assess the human health risks of OPFRs through inhalation by comparison with USEPA guidelines. On the basis of the estimated daily intake (EDI) of individual OPFR via inhalation, the HQ and CR were calculated using the reference dose (RfD) and the oral cancer slope factor (SFO), respectively. The calculation of each parameter is given in Eqs. (1)–(3):

$$HQ = EDI/RfD \quad (1)$$

$$EDI = (C \times IR \times IF \times T)/BW \quad (2)$$

where C is the concentration of $PM_{2.5}$-bound OPFR (pg/m^3); IR is the inhalation rate; T is the amount of time spent at work, and BW is the average body weight. Using the values in the exposure factor handbook of the Chinese population (adults) (Zhao and Duan, 2014), IR, T, and BW were set to 16.8 m^3/day, 1/3, and 67.4 kg, respectively. It was hypothesized that in the worst-case scenario, all $PM_{2.5}$-bound OPFRs were absorbed and utilized, i.e., IF was 100%. The RfD data are shown in Table S4. When the HQ was >1, there was a high likelihood of noncarcinogenic risk (Yue et al., 2022), otherwise the risk could be ignored.

The following formula was used to determine the CR of $PM_{2.5}$-bound OPFRs:

$$CR = EDI \times SFO \quad (3)$$

where SFO is the oral cancer slope factor (1/(ng/kg_{bw}/day), and it is listed in Table S4). When the CR was $>1 \times 10^{-6}$ there was a high lifetime risk of cancer development.

2.6. Statistical analysis

The SPSS 13 software (IBM, Armonk, NY, USA) was used for the statistical analysis. The Kruskal-Wallis test was applied to assess the substantial variations in target concentrations among the sample sites. Furthermore, the relationships between the concentrations were determined by a Spearman's correlation analysis. The outcomes were expressed as statistically significant correlations ($p < 0.05$) or strongly significant correlations ($p < 0.01$). The average value of parallel samples taken annually was used to calculate the OPFRs and $PM_{2.5}$ concentrations. According to Lu et al. (2018), C < LOD was classified as not detected, while LOD < C < LOQ was considered to be 1/4 LOQ (detection frequency <50%) or 1/2 LOQ (detection frequency ≥50%). A principal component analysis (PCA) with multiple linear regression (MLR) was conducted to determine the source of OPFRs.

3. Results and discussion

3.1. Seasonal variations of $PM_{2.5}$ concentrations

The $PM_{2.5}$ concentrations in the two parks and the control site are shown in Fig. 1. The $PM_{2.5}$ concentrations in the AP, MP, and BH were 47.2–175 (mean: 95.8 μg/m^3), 26.0–154 (mean: 83.6 μg/m^3), and 29.3–203 μg/m^3 (mean: 88.6 μg/m^3), respectively. There was no significant difference between the parks and the control site, which was attributed to the proactive and effective control measures undertaken by the government and the increased use of industrial dust removal equipment in recent years, both of which have positively contributed to the decrease in $PM_{2.5}$ pollution (State Council of the People's Republic of China, 2013; 2018). The measured values exceeded the secondary standard set by the China national standard GB3095-2012 (75 μg/m^3) by a factor ranging of 1.12–1.28 times, and the concentrations were 16.7–19.1 times the $PM_{2.5}$ limit value in the latest revised ""Global Air Quality Guidelines (2021) released by the World Health Organization (WHO). This demonstrates that the sampling sites had high concentrations of $PM_{2.5}$ contamination. Compared with previous studies, the present study recorded lower $PM_{2.5}$ concentrations than those recorded in Baotou (8.70–457 μg/m^3) (Zhou et al., 2016) and Xi'an (11.4–596 μg/m^3) (Yang et al., 2019), China. Although China's recent efforts to combat air pollution have had some success, the concentrations of $PM_{2.5}$ remain relatively high, and further strengthening of management measures is required.

Seasonal variations in $PM_{2.5}$ concentrations were observed, although there were no significant differences among the sites. In the AP, during winter and spring, the mean $PM_{2.5}$ concentrations surpassed the concentrations during summer and autumn. Comparable seasonal patterns were noted in the MP and BH. Similar seasonal trends on $PM_{2.5}$ were also observed in Xi'an, a city in northwest China (Ma et al., 2020; Yang et al., 2019). The fluctuations of $PM_{2.5}$ concentrations throughout the seasons could be attributed to both meteorological variables and human activities. For example, domestic heating in winter and spring promotes the generation of $PM_{2.5}$, especially in northern China. In Baotou, the rainy season extends from June to September, and is characterized by the heaviest precipitation of the year. This period of wet deposition through

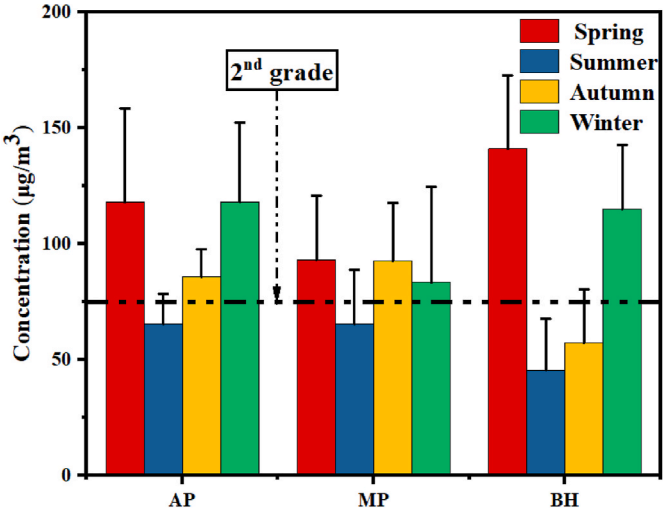

Fig. 1. The $PM_{2.5}$ concentration during the four seasons (the dashed line represents the 2nd grade of $PM_{2.5}$ concentration as defined by Chinese ambient air quality control criteria GB3095-2012).

rainfall effectively clears airborne particles. However, our study revealed a peak $PM_{2.5}$ concentration during spring, which contrasted with earlier findings (Ma et al., 2020; Yang et al., 2019). This may be due to frequent sandstorms during spring in Baotou (Zhou et al., 2016). Additionally, while the particle concentrations in summer and autumn did not significantly differ in the AP and MP, the concentrations were consistently higher than in the BH, suggesting that industrial derived $PM_{2.5}$ significantly contributed to the high concentrations. Furthermore, particle concentrations could also be influenced by other pollution sources, such as mobile sources (e.g., vehicle exhaust emissions).

3.2. The occurrence of OPFRs in $PM_{2.5}$ and seasonal variations

The OPFR concentrations in $PM_{2.5}$ from three locations were depicted in Fig. 2 and Table 1. Fifteen OPFRs were detected in $PM_{2.5}$ collected in Baotou throughout all four seasons, and the detection frequencies ranged from 42.9% to 100%, with the majority exceeding 80%. The results indicated that OPFRs are widely present in the atmospheric environment.

The OPFRs concentrations varied among the sampling areas (Table 1). The OPFRs concentrations ranged from 823 to 6.38×10^4 pg/m^3 (mean: 1.17×10^4 pg/m^3) in AP, from 12.4 to 6.67×10^3 pg/m^3 (mean: 852 pg/m^3) in MP, and from 167 to 8.98×10^3 pg/m^3 (mean: 1.51×10^3 pg/m^3) in the BH. The OPFRs concentrations in AP surpassed those in MP and BH, and the differences were statistically significant. In the AP, a recycling system for renewable resources was established, and scrap metal, electronic waste, rubber (plastic), and scrapped automobiles were reused or recycled. The higher OPFRs concentrations in the AP may be derived from the recycling of OPFRs-containing materials during industrial thermal processes. The OPFRs concentrations in the AP were comparable with those in Guangzhou (1.59×10^4 pg/m^3 and 1.35×10^4 pg/m^3) and Taiyuan (1.95×10^4 pg/m^3), in China (Chen et al., 2020), while they were higher than those in Beijing (1.84×10^3 pg/m^3) (Wang et al., 2018b), Dalian (1.20×10^3 pg/m^3) (Wang et al., 2020), Xinxiang (2.78×10^3 pg/m^3) (Yang et al., 2019), and Hong Kong (4.96×10^3 pg/m^3) (Wang et al., 2023) in China, and Cleveland (2.10×10^3 pg/m^3) and Chicago (1.50×10^3 pg/m^3) (Salamova et al., 2014) in the United States. The OPFRs concentrations in the MP were lower than those in the studies referred to above, primarily due to their singular usage in lubricating oils, which would leak or volatilize into atmosphere during metal deep processing activities (Kung et al., 2022; Liang et al., 2018). Meanwhile, OPFR levels are higher at BH than at MP because of the busy traffic and household activities in BH. The OPFRs concentrations in the BH were similar to those reported in previous studies conducted in cities (Wang et al., 2020; Wang et al., 2023). These results suggested that metal waste dismantling processes in the AP released relatively high concentrations of OPFRs, while there was only slight OPFRs pollution in the MP.

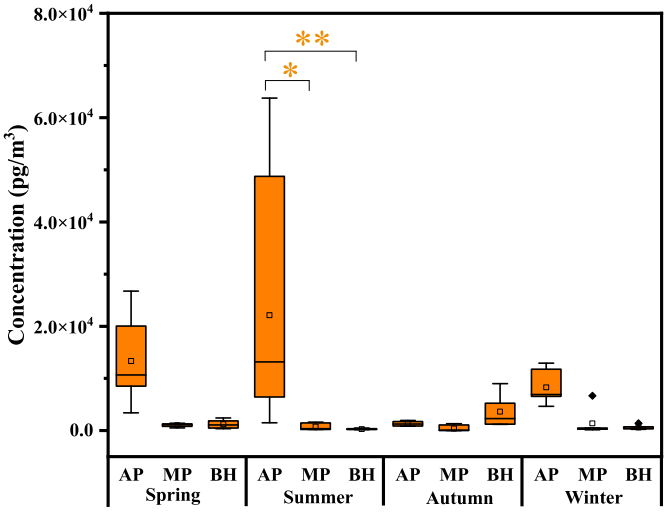

Fig. 2. Seasonal OPFRs concentrations in the three sites. *: The results were considered to be statistically significant at $p < 0.05$; **: The results were considered to be very statistically significant at $p < 0.01$.

Based on their chemical structures, OPFRs can be classified into chloro-, aryl-, and alkyl-substituted OPFRs, i.e., Cl-OPFRs, aryl-OPFRs, and alkyl-OPFRs, respectively. The mean Cl-OPFRs concentrations, including T (2-C)PP, TCPP, TDCPP, TCEP, and TCIPP, were 8.11×10^3 pg/m^3 in the AP, 438 pg/m^3 in the MP, and 1.14×10^3 pg/m^3 in the BH. The Cl-OPFRs concentrations in the AP were notably elevated compared to those in the MP ($p < 0.01$), which was potentially indicative of direct emissions from metal waste sources in the AP. Moreover, the Cl-OPFRs concentrations in the AP were comparable in magnitude to those previously documented in an e-cycling site in Islamabad, Pakistan (Faiz et al., 2018). The mean concentrations of aryl-OPFRs (EHDPP, *o*-TCP, *p*-TCP, *m*-TCP, and TPhP) were 216, 162, and 71.5 pg/m^3 in the AP, MP, and BH, respectively. The predominant aryl-OPFRs was EHDPP in AP because of its widespread use in paints and rubber, but the concentrations were lower than those observed in e-waste recycling areas in Pakistan (Iqbal et al., 2017) and Sweden (Wong et al., 2018), but higher than those observed in Hong Kong (Wang et al., 2023). The alkyl-OPFRs (TBOEP, TEHP, TEP, TBP, and TPrP) were detected with mean concentrations of 3.37×10^3 pg/m^3 in the AP, 252 pg/m^3 in the MP, and 298 pg/m^3 in the BH. There were statistically significant differences between the AP and MP/BH ($p < 0.01$), which suggested that the process of dismantling metal waste may be a significant source of alkyl-OPFRs.

There were different trends in the seasonal variations among the three sampling sites (Fig. 2). In the AP, the highest OPFRs concentration was recorded in summer ($2.21 \times 10^4 \pm 2.23 \times 10^4$ pg/m^3), followed by spring ($1.33 \times 10^4 \pm 7.76 \times 10^3$ pg/m^3), winter ($8.29 \times 10^3 \pm 2.99 \times 10^3$ pg/m^3), and autumn ($1.30 \times 10^3 \pm 411$ pg/m^3). In the MP, the mean concentration of $PM_{2.5}$-bound OPFRs was higher in winter ($1.38 \times 10^3 \pm 2.37 \times 10^3$ pg/m^3) and spring ($1.02 \times 10^3 \pm 295$ pg/m^3) than in autumn (357 ± 527 pg/m^3) and summer (722 ± 584 pg/m^3). In the BH, the mean concentration followed the descending order of autumn > spring > winter > summer, with values of 3.62×10^3, 1.21×10^3, 573, and 277 pg/m^3, respectively. The seasonal fluctuations observed in the MP could potentially be attributed to variations in meteorological conditions. Previous studies have suggested that the higher temperatures during warmer seasons may lead to the evaporation of semi-volatile compounds, subsequently enhancing the OPFRs concentrations in the gaseous phase and correspondingly reducing their concentrations in the particulate phase (Wang et al., 2006). Also, $PM_{2.5}$-bound OPFRs can be transported to the sampling site over long distances and the elevated $PM_{2.5}$ concentrations may increase the OPFRs concentrations. In addition to meteorological conditions and $PM_{2.5}$ concentrations, the OPFRs sources from various local production processes can also influence the concentrations. For example, the OPFRs concentrations in the AP were higher than those in the MP for each season, with a statistically significant increase in summer ($p < 0.05$). Moreover, in the AP and MP, the differences in OPFRs concentrations across seasons could be partly attributed to various industrial scenarios, such as adjustments in production schedules and temporary maintenance activities. For example, on March 9, 2021, the Development and Reform Commission of the Inner Mongolia Autonomous Region issued "Several Guarantee Measures for Ensuring the Completion of Energy Consumption Dual Control Target Tasks During the 14th Five-Year Plan Period", and implemented measures such as restricting energy consumption and imposing power cuts on key energy-consuming enterprises. Seasonal fluctuations in the OPFRs concentrations in the AP may correlate with the amount of metal recycling activities. In the BH, the OPFRs emissions arising from coal burning for heating purposes and from vehicle exhausts displayed seasonal variations. Overall, seasonal patterns of particle-bound OPFRs among three sampling sites were all affected by above factors, but the various intensity of each impact resulted in different trends in the

Table 1
Seasonal OPFRs concentrations (mean ± SD, pg/m^3) in the three sites.

Classification	Chemicals	Spring			Summer			Autumn			Winter		
		AP (n = 6)	MP (n = 7)	BH (n = 6)	AP (n = 7)	MP (n = 7)	BH (n = 6)	AP (n = 6)	MP (n = 7)	BH (n = 7)	AP (n = 6)	MP (n = 6)	BH (n = 6)
Cl-OPFRs	T (2-C)PP	508 ± 204	21.1 ± 0	37.3 ± 36.1	6.15 × 10^3 ± 6.64 × 10^3	11.8 ± 8.86	17.6 ± 7.88	188 ± 136	21.9 ± 45.5	976 ± 707	1.97 × 10^3 ± 1.02 × 10^3	36.0 ± 54.5	27.6 ± 25.1
	TCPP	402 ± 142	48.7 ± 16.7	33.4 ± 19.2	6.13 × 10^3 ± 7.04 × 10^3	24.7 ± 16.7	22.8 ± 12.8	113 ± 54.8	15.1 ± 24.4	1.16 × 10^3 ± 984	1.60 × 10^3 ± 1.00 × 10^3	87.4 ± 42.5	114 ± 168
	TDCPP	74.8 ± 111	20.7 ± 7.28	12.2 ± 8.42	75.8 ± 69.3	0	1.57 ± 3.52	42.3 ± 28.9	6.05 ± 10.1	22.3 ± 10.4	39.1 ± 10.7	120 ± 269	0
	TCEP	487 ± 181	193 ± 77.2	102 ± 31.9	2.97 × 10^3 ± 2.13 × 10^3	625 ± 535	123 ± 65.7	239 ± 116	81.9 ± 140	143 ± 66.3	587 ± 75.7	94.9 ± 43.0	111 ± 53.2
	TCIPP	569 ± 162	108 ± 21.9	112 ± 38.2	6.10 × 10^3 ± 6.77 × 10^3	24.8 ± 15.8	22.7 ± 10.1	182 ± 82.1	30.6 ± 50.1	1.03 × 10^3 ± 796	1.79 × 10^3 ± 965	194 ± 310	114 ± 154
∑Cl-OPFRs		2.04 × 10^3 ± 630	391 ± 103	297 ± 109	2.14 × 10^4 ± 2.20 × 10^4	687 ± 566	188 ± 79.4	764 ± 366	155 ± 264	3.33 × 10^3 ± 2.49 × 10^3	5.98 × 10^3 ± 2.97 × 10^3	533 ± 682	367 ± 391
Aryl-OPFRs	EHDPP	102 ± 54.7	64.8 ± 52.5	16.0 ± 13.0	77.4 ± 60.1	3.47 ± 1.47	4.22 ± 4.88	94.8 ± 84.9	5.09 ± 6.25	46.5 ± 72.3	245 ± 233	116 ± 241	6.41 ± 2.67
	TPhP	52.4 ± 22.9	93.6 ± 90.2	33.0 ± 10.8	106 ± 91.9	5.66 ± 3.87	3.65 ± 1.19	44.8 ± 15.4	16.2 ± 23.6	35.6 ± 12.9	122 ± 43.5	71.0 ± 139	7.46 ± 2.89
	o-TCP	0	5.36 ± 4.90	3.41 ± 7.48	0	3.19 ± 5.31	38.5 ± 80.3	0	0	0.07 ± 0.08	0.80 ± 1.79	138 ± 279	13.2 ± 18.0
	p-TCP	1.81 ± 2.38	7.45 ± 3.35	6.50 ± 7.89	0.66 ± 0.85	2.89 ± 3.83	17.4 ± 31.8	3.59 ± 5.00	1.00 ± 1.09	6.67 ± 8.01	3.50 ± 2.60	86.0 ± 140	10.5 ± 8.37
	m-TCP	3.83 ± 2.76	13.3 ± 8.97	8.08 ± 8.27	1.04 ± 1.26	3.30 ± 2.70	9.32 ± 14.2	5.07 ± 4.68	2.36 ± 2.63	7.92 ± 7.52	6.21 ± 1.93	50.9 ± 83.5	7.56 ± 4.19
∑Aryl-OPFRs		160 ± 74.0	185 ± 137	66.9 ± 41.4	185 ± 144	18.5 ± 15.9	73.0 ± 131	148 ± 80.6	24.6 ± 2.63	96.8 ± 81.4	378 ± 235	462 ± 881	45.2 ± 32.9
Alkyl-OPFRs	TBOEP	507 ± 477	17.6 ± 6.19	15.2 ± 6.64	204 ± 210	1.73 ± 2.73	0.23 ± 0.51	71.5 ± 49.9	4.35 ± 3.17	17.0 ± 17.0	345 ± 329	15.2 ± 30.2	2.66 ± 2.40
	TEHP	95.2 ± 46.6	61.1 ± 41.8	41.4 ± 18.8	58.4 ± 24.8	1.88 ± 1.11	3.25 ± 1.73	82.9 ± 29.3	11.4 ± 15.6	43.6 ± 39.3	134 ± 67.2	38.0 ± 80.4	4.46 ± 1.64
	TEP	1.05 × 10^4 ± 7.76 × 10^3	268 ± 205	625 ± 606	153 ± 160	11.8 ± 18.7	11.1 ± 13.6	81.6 ± 183	74.0 ± 118	56.9 ± 78.8	1.39 × 10^3 ± 1.04 × 10^3	173 ± 352	150 ± 192
	TBP	29.2 ± 20.0	97.8 ± 109	157 ± 235	87.9 ± 76.8	0.89 ± 0.75	0.98 ± 1.10	154 ± 65.6	85.8 ± 124	67.3 ± 17.6	53.1 ± 32.2	16.9 ± 35.6	0.59 ± 0.20
	TPrP	2.33 ± 1.88	2.52 ± 1.72	8.49 ± 10.3	0.49 ± 0.61	0.32 ± 0.64	0.84 ± 1.40	0.63 ± 0.60	1.86 ± 0.88	1.75 ± 0.88	2.58 ± 1.42	143 ± 309	2.68 ± 1.88
∑Alkyl-OPFRs		1.11 × 10^4 ± 7.80 × 10^3	447 ± 219	847 ± 667	504 ± 381	16.6 ± 21.0	16.4 ± 13.1	391 ± 181	177 ± 251	186 ± 120	1.92 × 10^3 ± 953	386 ± 807	160 ± 193
∑OPFRs		1.33 × 10^4 ± 7.76 × 10^3	1.02 × 10^3 ± 295	1.21 × 10^3 ± 732	2.21 × 10^4 ± 2.23 × 10^4	722 ± 584	277 ± 118	1.30 × 10^3 ± 411	357 ± 527	3.62 × 10^3 ± 2.65 × 10^3	8.29 × 10^3 ± 2.99 × 10^3	1.38 × 10^3 ± 2.37 × 10^3	573 ± 384

AP: an aluminum-processing industrial park; MP: a metal-fabrication industrial park; BH: a control site; T(2-C)PP: tris(2-chloropropyl) phosphate; TCPP: tris(chloropropyl) phosphate; TDCPP: tris(1,3-dichloro-2-propyl) phosphate; TCEP: tris(2-chloroethyl) phosphate; TCIPP: tris(2-chloroisopropyl) phosphate; EHDPP: 2-ethylhexyl diphenyl phosphate; TPhP: triphenyl phosphate; *o*-TCP: tri-*o*-cresyl phosphate; *p*-TCP: tri-*p*-cresyl phosphate; *m*-TCP:tri-*m*-cresyl phosphate; TBOEP: tris(2-butoxyethyl) phosphate; TEHP: tris(2-ethylhexyl) phosphate; TEP: tetraethyl diphosphate; TBP: tributyl phosphate; TPrP: tripropyl phosphate.

seasonal variations.

3.3. Composition profiles and sources of $PM_{2.5}$-bound OPFRs

To explore the sources of $PM_{2.5}$-bound OPFRs, compositional characteristics of detected OPFRs were studied. As show in Fig. 3, the predominant homologues of OPFRs varied at the different sampling sites. The Cl-OPFRs accounted for a relatively high proportion of total OPFRs in all locations; i.e., 69.3%, 51.4%, and 75.5% of the total OPFRs in the AP, MP, and BH, respectively. The alkyl-OPFRs were the second most prevalent group of contaminants, accounting for 28.8%, 29.6%, and 19.8% of all OPFRs in the three sampling sites, respectively. It is common for Cl-OPFRs to be used as additives for flame retardancy and plasticizing in electronic components, car accessories, automotive interiors, and rubber products (Song et al., 2024). These chemicals are the most widely used type of OPFRs at the global scale, constituting a

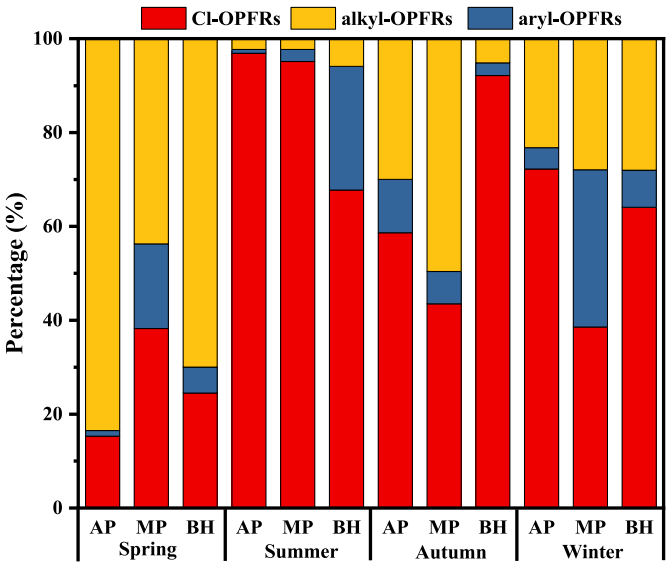

Fig. 3. Compositional profiles of individual OPFRs in the three sites during one year.

significant 24.0% share of all OPFRs manufactured in 2020 (Kung et al., 2022). In addition to their high usage, Cl-OPFRs exhibit resistance to atmospheric transformation (for example, via alkaline hydrolysis or photodegradation) due to their chloro-substituted structure, contributing to their relatively persistent nature (Na et al., 2020; Zeng et al., 2021). Correspondingly, some non-Cl-OPFRs containing ester bonds may undergo hydrolysis reactions in a humid atmospheric environment, generating corresponding acids and alcohols. Therefore, Cl-OPFRs was the predominant homologue, although the individual Cl-OPFR compounds differed among the sites. For example, T (2-C)PP (20.2%), and TCPP (19.0%) were predominant in the AP, while TCEP (29.9%), and TCIPP (10.0%) were predominant in the MP, and TCPP (24.3%), and T (2-C)PP (19.4%) were predominant in the BH (Fig. S1). The dominant status of Cl-OPFRs was also apparent in a study conducted in the Beijing−Tianjin−Hebei region of China because of their extensive usage (Zhang et al., 2020). Therefore, the composition profiles of $PM_{2.5}$-bound OPFRs at different sites might be affected by the type of OPFR usage and the behaviors of the chemicals in the environment.

Although Cl-OPFRs were the predominant homologue at all three sites, there were seasonal variations in the sites as shown in Fig. 3. In the AP, alkyl-OPFRs (83.5%) accounted for the highest proportion in spring, while Cl-OPFRs were predominant in summer, autumn, and winter (96.9%, 58.7%, and 72.2%, respectively). Similar results were found in the BH, where the dominant OPFR compounds were alkyl-OPFRs during spring (70.0%), while Cl-OPFRs were dominant in summer (67.8%), autumn (92.2%), and winter (64.1%). In the MP, alkyl-OPFRs were the prevalent homologue in both spring (43.7%) and autumn (49.6%), while Cl-OPFRs were the most abundant in summer (95.1%) and winter (38.6%). The composition profiles of OPFRs in $PM_{2.5}$ were influenced by a range of factors, including their physicochemical attributes, emission sources, and prevailing meteorological conditions. For example, in spring, alkyl-OPFRs were the prevalent homologue among three sampling sites. In agricultural production surrounding Baotou, the widely used pesticides and acaricides contains alkyl-OPFRs, such as TEP. The alkyl-OPFRs in soils are transported to the urban area of Baotou along with the airflow of sandstorms. Except for their slightly lower abundance compared to alkyl-OPFRs in autumn in the MP, Cl-OPFRs were predominant in the three sampling sites in summer, autumn, and winter because of their high rate of production and extensive usage, e.g., electronics, furniture foams, and plasticizers in rubber products (Li et al., 2019). In addition, the highly polar Cl-OPFRs are more likely to have strong electrostatic interactions or polar interactions with the polar parts on the surface of particulate matter, thus being more easily adsorbed on particulate matter.

To identify the sources of OPFRs, the correlations among individual compounds were analyzed (Fig. 4). In the AP, significant correlations ($p < 0.05$) were observed among the dominant Cl-OPFRs. There was a positive correlation between TCPP and each of T (2-C)PP, TCEP, and TCIPP. The strong correlations between TCEP and TCPP could be largely explained by their similar applications (e.g., paint and coating, thermoplastics) and physicochemical properties (e.g., vapor pressure or log K_{OW}). The same results were also reported in the U.S.A. and southern Chinese cities (Clark et al., 2017; Zeng et al., 2021). In the MP, except for TCEP and TBP, there were statistically significant positive relationships among the OPFRs ($p < 0.05$). The correlations among the OPFRs in the MP were attributed to there being similar sources. The strong correlations between individual OPFRs were comparable to those reported in atmospheric particulate matter from Silesia, Poland (Fabianska et al., 2019). In the BH, significant positive correlations were found among some OPFRs ($p < 0.05$). However, for most substances, there were no discernible associations ($p > 0.05$), suggesting complex pollution sources or other contributing factors that might impact OPFRs production.

To further explore the potential OPFRs emission sources and quantify their proportional contributions, a PCA with MLR was conducted among the industrial parks (Table S3). It was found that PC1, PC2, PC3, and PC4 explained 36.3%, 26.5%, 11.9%, and 11.6% of the total variance, and contributed 2.85%, 68.0%, 3.82%, and 25.3% of the total OPFRs, respectively. PC1 was dominated by TPrP, *o*-TCP, *p*-TCP, and *m*-TCP. These substances are frequently used in industrial machinery as engine oils, hydraulic fluids, and cutting fluids for a variety of electrical devices (Hu et al., 2021). For example, leaked hydraulic oil will quickly volatilize by high temperatures into the atmosphere. PC2 was mainly loaded with T (2-C)PP, TCIPP, TCPP, and TCEP. Waste recycling processes are the primary sources of these Cl-OPFRs. For example, the prevalence of baking or burning of plastics and printed wiring boards resulted in widespread Cl-OPFRs contamination. A trend observed in metal waste recycling regions in both China and Pakistan (Faiz et al., 2018; Wang et al., 2018a). PC3 consisted primarily of TBP, which is typically used for its adhesive and flame-resistant properties in construction-related substances (Zeng et al., 2021). TBP can slowly migrate into the atmosphere from the building materials over time, and the migration and evaporation of flame retardants may be enhanced in areas with high humidity or temperature fluctuations. PC4 was mainly associated with TBOEP and TEP. As reported in the literature, TBOEP is an essential component of coverings, lubricants, and hydraulic liquids, and it may also be abrasive and emit off-gas from devices and machines (Luo et al., 2020). Additionally, TEP is also used as a monitor of engine exhausts powered by gasoline (Chen et al., 2020; Hu et al., 2021). These four main components explained 86.3% of the total variance in OPFR concentrations in AP and MP. This indicates that in addition to several major sources of OPFRs, there are also some minor sources, including long-distance transmission, photochemical reaction and oxidation reaction. Therefore, many waste recycling facilities in AP are maximal sources of OPFRs.

3.4. Potential human health risk assessment

With the rapid growth in the use of OPFRs, many studies have shown that there are concerning human health risks from the chemicals (Li et al., 2022; Rosenmai et al., 2021). To estimate the human intake and the associated health risks of OPFRs, for each OPFR the EDI and HQ were calculated, with the results shown in Table 2. A high exposure was represented by the 95th percentile of the EDI. Across sampling locations, the mean and 95th percentiles of the EDI were in the range of 1.60×10^{-5}–0.24 and 2.80×10^{-4}–1.82 ng/kg_{bw}/day, respectively. The OPFRs EDIs through inhalation were far lower than their RfDs. As a result, the risks from OPFRs showed that the HQ values ranged from 6.47×10^{-8}–2.14×10^{-4}, and the maximum HQ was likewise significantly less

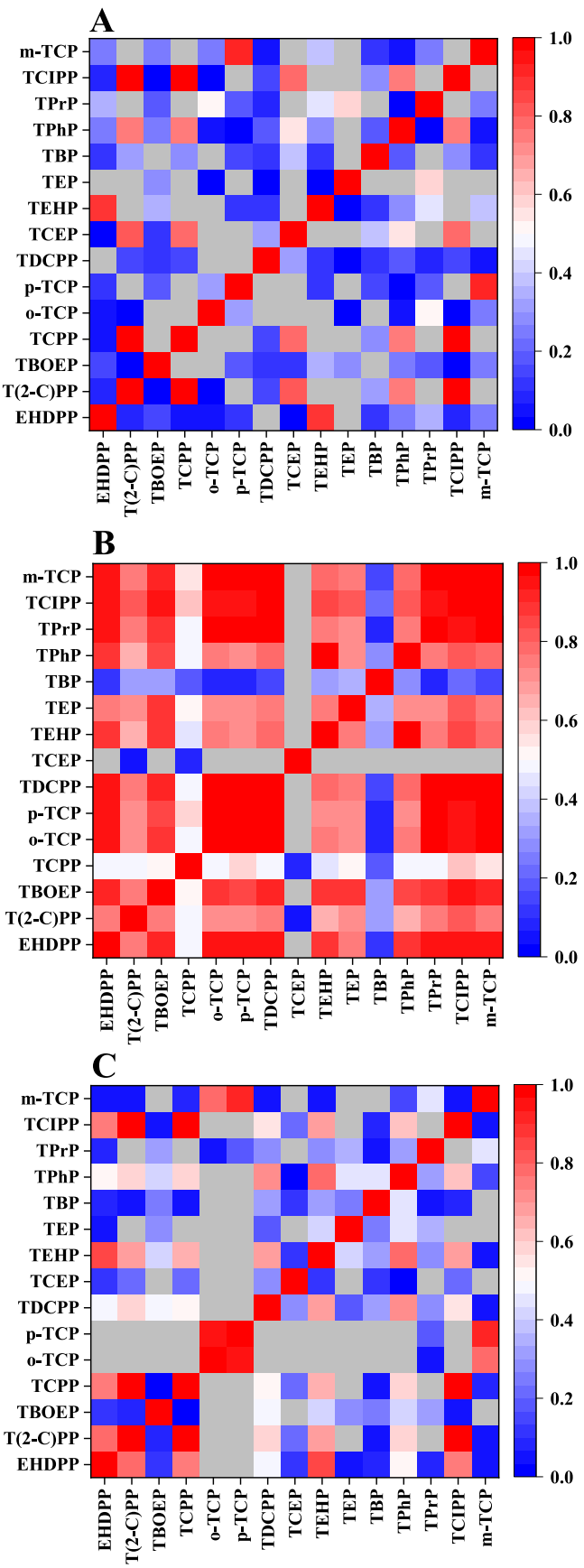

Fig. 4. Spearman correlation heat maps of OPFRs in (A) an aluminum-processing industrial park (AP), (B) a metal-fabrication industrial park (MP), and (C) a control site (BH).

than the threshold value of 1 in the worst case. The results indicated that the non-carcinogenic risk following exposure to particulate OPFRs in Baotou could be disregarded. Comparatively, there was a higher risk in industrial areas than in residential areas. The risk followed the sequence of AP > MP > BH for the three sampling sites. For the different types of OPFRs, Cl-OPFRs accounted for 91.5% of the non-carcinogenic risk for workers in the two parks under the worst-case scenario, with 53.3% from TCIPP and 32.7% from TCEP. The significantly greater HQs of TCIPP and TCEP were ascribed to their higher ambient concentrations and lower RfD values. Previous studies have shown that TCIPP and TCEP are non-carcinogenic but exposure can lead to liver toxicity, reproductive toxicity, and neurotoxicity (Deepika et al., 2023). Therefore, these chemicals are still a cause for concern in the environment.

To further understand the health risk from OPFRs in $PM_{2.5}$, the carcinogenic risk was also considered. The CR results for the various OPFRs are shown in Fig. S2. The total CR values ranged from 4.28×10^{-12} to 1.25×10^{-8}, which were all beneath the limit value of 1×10^{-6} in the current exposure scenarios. Analogous to the non-carcinogenic risks, the risk followed the sequence of AP > MP > BH, indicating that there was a higher carcinogenic risk in industrial areas. Among the target OPFRs, TCEP accounted for 92.5% of the CR index for workers in the two parks under the high exposure scenario. There is evidence to suggest that TCEP has a potential carcinogenic risk on a basis of physiologically based kinetic model in rats (Deepika et al., 2023).

Two toxic endpoints were considered in the human health risk assessment in the present study. However, there were several uncertainties. First, the current data on OPFRs remains very limited. The RfD used here was an oral reference dose for individual OPFRs. Currently, there is a lack of reference doses for the respiratory intake of OPFRs. Different exposure pathways, such as inhalation, oral intake, and skin contact, have different routes into the bloodstream and encounter varying enzymatic actions, leading to diverse impacts on the human body. Second, as a semi volatile substance, some OPFRs exist in the atmosphere in a gaseous form. Therefore, the risk of OPFRs exposure through inhalation was likely underestimated, especially for the more volatile OPFRs. Third, a portion of the inhaled atmospheric particulate matter can be expelled from the body in the process of gaseous exchange during inhalation. Therefore, breathing in airborne OPFRs does not completely absorb them, reducing the risk to human health. Fourth, the lack of SFO data for the other OPFRs that may be carcinogenic could cause the overall CR value of human exposure to particulate OPFRs to be underestimated. Therefore, there remains a substantial amount of research needed to comprehensively investigate the health risks posed by OPFRs.

4. Conclusions

This study has made significant contributions to understanding the presence and seasonal characteristics of $PM_{2.5}$-bound OPFRs in industrial parks dedicated to aluminum products and metal deep processing. The findings revealed that Seasonal variations of $PM_{2.5}$ and OPFRs were within specific ranges, with the aluminum-processing industrial park having higher OPFR concentrations than the metal-fabrication industrial park. The Cl-OPFRs (e.g., TCEP and TCPP) were the dominant homologue among the three sampling sites because of their extensive usage and chemical stability. The primary source of OPFRs was the disposal of metal wastes, especially for Cl-OPFRs. The health risk assessment showed that the $PM_{2.5}$-bound OPFRs did not lead to an obvious risk when considering both non-carcinogenic and carcinogenic endpoints, although Cl-OPFRs presented a relatively higher risk than the other OPFRs. In conclusion, this research has provided valuable insights into the environmental pollution caused by OPFRs in metal-related industrial parks. Future studies could expand the scope of research to include more industrial parks and explore more effective measures to reduce OPFR emissions and mitigate potential health risks.

Table 2
The estimated daily intakes of OPFRs (ng/kg_{bw}/day) and the maximum HQ via inhalable $PM_{2.5}$.

Classification	Chemicals	EDI						HQ ($\times 10^{-3}$)		
		AP (n = 25)		MP (n = 27)		BH (n = 25)		AP (n = 25)	MP (n = 27)	BH (n = 25)
		Mean	95th	Mean	95th	Mean	95th	Maximum	Maximum	Maximum
Cl-OPFRs	T (2-C)PP	0.20	1.44	1.85×10^{-3}	0.01	0.02	0.18	–	–	–
	TCPP	0.18	1.51	3.52×10^{-3}	0.01	0.03	0.22	–	–	–
	TDCPP	4.88×10^{-3}	0.02	2.80×10^{-3}	0.04	7.94×10^{-4}	3.01×10^{-3}	5.37×10^{-3}	0.01	6.59×10^{-4}
	TCEP	0.10	0.53	0.02	0.11	0.01	0.02	0.09	0.02	3.18×10^{-3}
	TCIPP	0.19	1.47	7.09×10^{-3}	0.08	0.03	0.19	0.16	7.35×10^{-3}	0.02
∑Cl-OPFRs		0.67	4.84	0.04	0.15	0.09	0.61	0.26	0.04	0.03
Aryl-OPFRs	EHDPP	0.01	0.05	3.73×10^{-3}	0.04	1.61×10^{-3}	0.01	4.21×10^{-3}	3.63×10^{-3}	1.23×10^{-3}
	TPhP	6.85×10^{-3}	0.02	3.80×10^{-3}	0.03	1.71×10^{-3}	4.50×10^{-3}	3.53×10^{-4}	4.53×10^{-4}	6.45×10^{-5}
	o-TCP	1.60×10^{-5}	2.80×10^{-4}	2.72×10^{-3}	0.04	1.10×10^{-3}	0.01	3.08×10^{-5}	4.86×10^{-3}	1.39×10^{-3}
	p-TCP	1.93×10^{-4}	1.00×10^{-3}	1.83×10^{-3}	0.02	8.41×10^{-4}	5.78×10^{-3}	8.92×10^{-5}	2.52×10^{-3}	5.64×10^{-4}
	m-TCP	3.26×10^{-4}	1.05×10^{-3}	1.35×10^{-3}	0.01	6.82×10^{-4}	3.02×10^{-3}	9.22×10^{-5}	1.51×10^{-3}	2.60×10^{-4}
∑Aryl-OPFRs		0.02	0.06	0.01	0.14	5.94×10^{-3}	0.03	4.78×10^{-3}	0.01	3.52×10^{-3}
Alkyl-OPFRs	TBOEP	0.02	0.10	7.89×10^{-4}	4.94×10^{-3}	7.56×10^{-4}	3.94×10^{-3}	7.65×10^{-3}	4.57×10^{-4}	3.16×10^{-4}
	TEHP	7.58×10^{-3}	0.02	2.30×10^{-3}	0.02	1.99×10^{-3}	9.58×10^{-3}	2.21×10^{-4}	1.81×10^{-4}	1.13×10^{-4}
	TEP	0.24	1.82	0.01	0.07	0.02	0.13	–	–	–
	TBP	6.75×10^{-3}	0.02	4.29×10^{-3}	0.03	4.72×10^{-3}	0.04	2.21×10^{-3}	3.01×10^{-3}	5.64×10^{-3}
	TPrP	1.22×10^{-4}	4.42×10^{-4}	2.74×10^{-3}	0.04	2.80×10^{-4}	1.95×10^{-3}	–	–	–
∑Alkyl-OPFRs		0.28	1.88	0.02	0.13	0.02	0.15	0.01	3.65×10^{-3}	6.07×10^{-3}
∑OPFRs		0.97	4.92	0.07	0.39	0.13	0.65	0.27	0.05	0.03

AP: an aluminum-processing industrial park; MP: a metal-fabrication industrial park; BH: a control site; T(2-C)PP: tris(2-chloropropyl) phosphate; TCPP: tris(chloropropyl) phosphate; TDCPP: tris(1,3-dichloro-2-propyl) phosphate; TCEP: tris(2-chloroethyl) phosphate; TCIPP: tris(2-chloroisopropyl) phosphate; EHDPP: 2-ethylhexyl diphenyl phosphate; TPhP: triphenyl phosphate; *o*-TCP: tri-*o*-cresyl phosphate; *p*-TCP: tri-*p*-cresyl phosphate; *m*-TCP:tri-*m*-cresyl phosphate; TBOEP: tris(2-butoxyethyl) phosphate; TEHP: tris(2-ethylhexyl) phosphate; TEP: tetraethyl diphosphate; TBP: tributyl phosphate; TPrP: tripropyl phosphate.

CRediT authorship contribution statement

Helong Ren: Writing – original draft, Methodology, Data curation. **Qiang Chen:** Writing – original draft, Supervision, Conceptualization. **Zhaofa Huang:** Methodology. **Yuhuan Zhu:** Methodology. **Jing She:** Methodology. **Yingxin Yu:** Writing – review & editing, Supervision, Conceptualization.

Declaration of competing interest

The authors declare that they have no known competing financial interests or personal relationships that could have appeared to influence the work reported in this paper.

Acknowledgments

The study was supported by the National Natural Science Foundation of China (41991311), and Guangdong Provincial Key R&D Program (2022-GDUT-A0007), the Local Innovative and Research Teams Project of Guangdong Pearl River Talents Program (2017BT01Z032), and Guangdong-Hong Kong-Macao Joint Laboratory for Contaminants Exposure and Health (2020B1212030008).

Appendix A. Supplementary data

Supplementary data to this article can be found online at https://doi.org/10.1016/j.envpol.2024.125212.

Data availability

The data that has been used is confidential.

References

Bekele, T.G., Zhao, H.X., Wang, Q.Z., Chen, J.W., 2019. Bioaccumulation and trophic transfer of emerging organophosphate flame retardants in the marine food webs of Laizhou Bay, North China. Environ. Sci. Technol. 53 (22), 13417–13426.

Chen, Y.Y., Song, Y.Y., Chen, Y.J., Zhang, Y.H., Li, R.J., Wang, Y.J., Qi, Z.H., Chen, Z.F., Cai, Z.W., 2020. Contamination profiles and potential health risks of organophosphate flame retardants in $PM_{2.5}$ from Guangzhou and Taiyuan, China. Environ. Int. 134, 105343.

Clark, A.E., Yoon, S., Sheesley, R.J., Usenko, S., 2017. Spatial and temporal distributions of organophosphate ester concentrations from atmospheric particulate matter samples collected across Houston, TX. Environ. Sci. Technol. 51 (8), 4239–4247.

Deepika, D., Sharma, R.P., Schuhmacher, M., Kumar, V., 2023. Development of a rat physiologically based kinetic model (PBK) for three organophosphate flame retardants (TDCIPP, TCIPP, TCEP). Toxicol. Lett. 383, 128–140.

Fabianska, M.J., Kozielska, B., Konieczynski, J., Bielaczyc, P., 2019. Occurrence of organic phosphates in particulate matter of the vehicle exhausts and outdoor environment - a case study. Environ. Pollut. 244, 351–360.

Faiz, Y., Siddique, N., He, H., Sun, C., Waheed, S., 2018. Occurrence and profile of organophosphorus compounds in fine and coarse particulate matter from two urban areas of China and Pakistan. Environ. Pollut. 233, 26–34.

Ge, X., Ma, S.T., Huo, Y.P., Yang, Y., Luo, X.J., Yu, Y.X., An, T.C., 2022. Mixed bromine/chlorine transformation products of tetrabromobisphenol A: potential specific molecular markers in e-waste dismantling areas. J. Hazard Mater. 423, 127126.

Ge, X., Ma, S.T., Zhang, X.L., Yang, Y., Li, G.Y., Yu, Y.X., 2020. Halogenated and organophosphorous flame retardants in surface soils from an e-waste dismantling park and its surrounding area: distributions, sources, and human health risks. Environ. Int. 139, 105741.

Hu, Z.H., Yin, L.S., Wen, X.F., Jiang, C.B., Long, Y.N., Zhang, J.W., Liu, R.Y., 2021. Organophosphate esters in China: fate, occurrence, and human exposure. Toxics 9 (11), 310.

Iqbal, M., Syed, J.H., Breivik, K., Chaudhry, M.J.I., Li, J., Zhang, G., Malik, R.N., 2017. E-waste driven pollution in Pakistan: the first evidence of environmental and human exposure to flame retardants (FRs) in Karachi city. Environ. Sci. Technol. 51 (23), 13895–13905.

Kim, U.J., Wang, Y., Li, W.H., Kannan, K., 2019. Occurrence of and human exposure to organophosphate flame retardants/plasticizers in indoor air and dust from various microenvironments in the United States. Environ. Int. 125, 342–349.

Kung, H.C., Hsieh, Y.K., Huang, B.W., Cheruiyot, N.K., Chang-Chien, G.P., 2022. An overview: organophosphate flame retardants in the atmosphere. Aerosol Air Qual. Res. 22 (7), 220148.

Li, W.H., Wang, Y., Asimakopoulos, A.G., Covaci, A., Gevao, B., Johnson-Restrepo, B., Kumosani, T.A., Malarvannan, G., Moon, H.B., Nakata, H., Sinha, R.K., Tran, T.M., Kannan, K., 2019. Organophosphate esters in indoor dust from 12 countries: concentrations, composition profiles, and human exposure. Environ. Int. 133, 105178.

Li, X.J., Li, Q., Zhou, J.H., Guo, C.S., Zhong, N., Yu, Y.X., 2022. Urinary metabolites of organophosphorus flame retardants in Guangzhou population: exposure and health risk. China Environ. Sci. 42 (3), 1410–1417.

Li, Y.T., Wang, X., Zhu, Q.Q., Xu, Y.Q., Fu, Q.G., Wang, T., Liao, C.Y., Jiang, G.B., 2023. Organophosphate flame retardants in pregnant women: sources, occurrence, and potential risks to pregnancy outcomes. Environ. Sci. Technol. 57 (18), 7109–7128.

Liang, Z.R., Chen, L.F., Alam, M.S., Rezaei, S.Z., Stark, C., Xu, H.M., Harrison, R.M., 2018. Comprehensive chemical characterization of lubricating oils used in modern vehicular engines utilizing GC × GC-TOFMS, Fuel, 220, 792–799.
Lu, Q.O., Jung, C.C., Chao, H.R., Chen, P.S., Lee, C.W., Tran, Q.T.P., Ciou, J.Y., Chang, W.H., 2023. Investigating the associations between organophosphate flame retardants (OPFRs) and fine particles in paired indoor and outdoor air: a probabilistic prediction model for deriving OPFRs in indoor environments. Environ. Int. 174, 107871.
Lu, S.Y., Kang, L., Liao, S.C., Ma, S.T., Zhou, L., Chen, D.Y., Yu, Y.X., 2018. Phthalates in $PM_{2.5}$ from Shenzhen, China and human exposure assessment factored their bioaccessibility in lung. Chemosphere 202, 726–732.
Luo, Q., Gu, L.Y., Wu, Z.P., Shan, Y., Wang, H., Sun, L.N., 2020. Distribution, source apportionment and ecological risks of organophosphate esters in surface sediments from the Liao River, Northeast China. Chemosphere 250, 126297.
Ma, B.B., Wang, L.J., Tao, W.D., Liu, M.M., Zhang, P.Q., Zhang, S.W., Li, X.P., Lu, X.W., 2020. Phthalate esters in atmospheric $PM_{2.5}$ and PM_{10} in the semi-arid city of Xi'an, Northwest China: pollution characteristics, sources, health risks, and relationships with meteorological factors. Chemosphere 242, 125226.
Ma, S.T., Yue, C.C., Tang, J., Lin, M.Q., Zhuo, M.H., Yang, Y., Li, G.Y., An, T.C., 2021. Occurrence and distribution of typical semi-volatile organic chemicals (SVOCs) in paired indoor and outdoor atmospheric fine particle samples from cities in southern China. Environ. Pollut. 269, 116123.
Montone, R.A., Rinaldi, R., Bonanni, A., Severino, A., Pedicino, D., Crea, F., Liuzzo, G., 2023. Impact of air pollution on ischemic heart disease: evidence, mechanisms, clinical perspectives. Atherosclerosis 366, 22–31.
Na, G.S., Hou, C., Li, R.J., Shi, Y.L., Gao, H., Jin, S.C., Gao, Y.Z., Jiao, L.P., Cai, Y.Q., 2020. Occurrence, distribution, air-seawater exchange and atmospheric deposition of organophosphate esters (OPEs) from the northwestern Pacific to the Arctic Ocean. Mar. Pollut. Bull. 157, 111243.
Ren, H.L., Ge, X., Qi, Z.H., Lin, Q.H., Shen, G.F., Yu, Y.X., An, T.C., 2023. Emission and gas-particle partitioning characteristics of atmospheric halogenated and organophosphorus flame retardants in decabromodiphenyl ethane-manufacturing functional areas. Environ. Pollut. 329, 121709.
Research In China, 2014. Global and China Flame Retardant Industry Report, pp. 2014–2016. Htmls/Report/2014/7904.html.
Rosenmai, A.K., Winge, S.B., Moller, M., et al., 2021. Organophosphate ester flame retardants have antiandrogenic potential and affect other endocrine related endpoints in vitro and in silico. Chemosphere 263, 127703.
Salamova, A., Ma, Y.N., Venier, M., Hites, R.A., 2014. High concentrations of organophosphate flame retardants in the Great Lakes atmosphere. Environ. Sci. Technol. Lett. 1 (1), 8–14.
Sanchez-Pinero, J., Novo-Quiza, N., Pernas-Castano, C., Moreda-Pineiro, J., Muniategui-Lorenzo, S., Lopez-Mahia, P., 2022. Inhalation bioaccessibility of multi-class organic pollutants associated to atmospheric $PM_{2.5}$: correlation with $PM_{2.5}$ properties and health risk assessment. Environ. Pollut. 307, 119577.
Song, X.W., Zhu, S., Hu, L., Chen, X.J., Zhang, J.Q., Liu, Y., Bu, Q.W., Ma, Y.N., 2024. A review of the distribution and health effect of organophosphorus flame retardants in indoor environments. Toxics 12 (3), 195.
State Council of the People's Republic of China, 2013. Action Plan for Prevention and Control of Air Pollution.
State Council of the People's Republic of China, 2018. Three-year Action Plan to Win the Battle for a Blue Sky.
Sühring, R., Diamond, M.L., Scheringer, M., Wong, F., Pućko, M., Stern, G., Burt, A., Hung, H., Fellin, P., Li, H., Jantunen, L.M., 2016. Organophosphate esters in Canadian Arctic air: occurrence, concentrations and trends. Environ. Sci. Technol. 50 (14), 7409–7415.
Tansel, B., 2017. From electronic consumer products to e-wastes: global outlook, waste quantities, recycling challenges. Environ. Int. 98, 35–45.
Thangavel, P., Park, D., Lee, Y.C., 2022. Recent insights into particulate matter ($PM_{2.5}$)-mediated toxicity in humans: an overview. Int. J. Environ. Res. Publ. Health 19, 7511.
Van den Eede, N., Dirtu, A.C., Neels, H., Covaci, A., 2011. Analytical developments and preliminary assessment of human exposure to organophosphate flame retardants from indoor dust. Environ. Int. 37 (2), 454–461.
Wang, T., Ding, N., Wang, T., Chen, S.J., Luo, X.J., Mai, B.X., 2018a. Organophosphorus esters (OPEs) in $PM_{2.5}$ in urban and e-waste recycling regions in southern China: concentrations, sources, and emissions. Environ. Res. 167, 437–444.
Wang, T., Tian, M., Ding, N., Yan, X., Chen, S.J., Mo, Y.Z., Yang, W.Q., Bi, X.H., Wang, X. M., Mai, B.X., 2018b. Semivolatile organic compounds (SOCs) in fine particulate matter ($PM_{2.5}$) during clear, fog, and haze episodes in winter in Beijing, China. Environ. Sci. Technol. 52 (9), 5199–5207.
Wang, X.M., Leung, C.W., Cai, Z.W., Hu, D., 2023. $PM_{2.5}$-bound organophosphate flame retardants in Hong Kong: occurrence, origins, and source-specific health risks. Environ. Sci. Technol. 57 (38), 14289–14298.
Wang, Y., Bao, M.J., Tan, F., Qu, Z.P., Zhang, Y.W., Chen, J.W., 2020. Distribution of organophosphate esters between the gas phase and $PM_{2.5}$ in urban Dalian, China. Environ. Pollut. 259, 113882.
Wang, Y., Zhuang, G.S., Zhang, X.Y., Huang, K., Xu, C., Tang, A.H., Chen, J.M., An, Z.S., 2006. The ion chemistry, seasonal cycle, and sources of $PM_{2.5}$ and TSP aerosol in Shanghai. Atmos. Environ. 40 (16), 2935–2952.
Wong, F., de Wit, C.A., Newton, S.R., 2018. Concentrations and variability of organophosphate esters, halogenated flame retardants, and polybrominated diphenyl ethers in indoor and outdoor air in Stockholm, Sweden. Environ. Pollut. 240, 514–522.
Yang, J., Yao, Y.M., Li, X.X., He, A., Chen, S.J., Wang, Y.L., Dong, X.Y., Chen, H., Wang, Y., Wang, L., Sun, H.W., 2024. Nontarget identification of novel organophosphorus flame retardants and plasticizers in indoor air and dust from multiple microenvironments in China. Environ. Sci. Technol. 58 (18), 7986–7997.
World Health Organization, 2021. Global Air Quality Guidelines. https://www.who.int/publications/i/item/9789240034228.
Yang, K., Li, Q.L., Yuan, M., Guo, M.R., Wang, Y.Q., Li, S.Y., Tian, C.G., Tang, J.H., Sun, J.H., Li, J., Zhang, G., 2019. Temporal variations and potential sources of organophosphate esters in $PM_{2.5}$ in Xinxiang, North China. Chemosphere 215, 500–506.
Yue, C.C., Ma, S.T., Liu, R.R., Yang, Y., Li, G.Y., Yu, Y.X., An, T.C., 2022. Pollution profiles and human health risk assessment of atmospheric organophosphorus esters in an e-waste dismantling park and its surrounding area. Sci. Total Environ. 806 (3), 151206.
Zeng, Y., Chen, S.J., Liang, Y.H., Zhu, C.Y., Liu, Z., Guan, Y.F., Ma, H.M., Mai, B.X., 2021. Traditional and novel organophosphate esters (OPEs) in $PM_{2.5}$ of a megacity, southern China: spatioseasonal variations, sources, and influencing factors. Environ. Pollut. 284, 117208.
Zhang, S., Li, H.L., He, R.J., Deng, W.Q., Ma, S.T., Zhang, X., Li, G.Y., An, T.C., 2023. Spatial distribution, source identification, and human health risk assessment of PAHs and their derivatives in soils nearby the coke plants. Sci. Total Environ. 861, 160588.
Zhang, W.W., Wang, P., Zhu, Y., Wang, D., Yang, R.Q., Li, Y.M., Matsiko, J., Zuo, P.J., Qin, L., Yang, X., Zhang, Q.H., Jiang, G.B., 2020. Occurrence and human exposure assessment of organophosphate esters in atmospheric $PM_{2.5}$ in the Beijing-Tianjin-Hebei region, China. Ecotoxicol. Environ. Saf. 206, 111399.
Zhao, S.Z., Tian, L.L., Zou, Z.H., Liu, X., Zhong, G.C., Mo, Y.Z., Wang, Y., Tian, Y.K., Li, J., Guo, H., Zhang, G., 2021. Probing legacy and alternative flame retardants in the air of Chinese cities. Environ. Sci. Technol. 55 (14), 9450–9459.
Zhao, X.G., Duan, X.L., 2014. Exposure factors handbook of Chinese population (adults). China Environ. Sci. Press. https://xueshu.baidu.com/usercenter/paper/show?paperid=e465457384e7dac4d9d463f96ff08600&site=xueshu_se.
Zhong, W.J., Cui, Y.N., Li, R.X., Yang, R.Y., Li, Y., Zhu, L.Y., 2021. Distribution and sources of ordinary monomeric and emerging oligomeric organophosphorus flame retardants in Haihe Basin. China. Sci. Total Environ. 785, 147274.
Zhou, H.J., He, J., Zhao, B.Y., Zhang, L.J., Fan, Q.Y., Lü, C.W., Dudagula, Liu, T., Yuan, Y. H., 2016. The distribution of PM_{10} and $PM_{2.5}$ carbonaceous aerosol in Baotou, China. Atmos. Res. 178, 102–113.